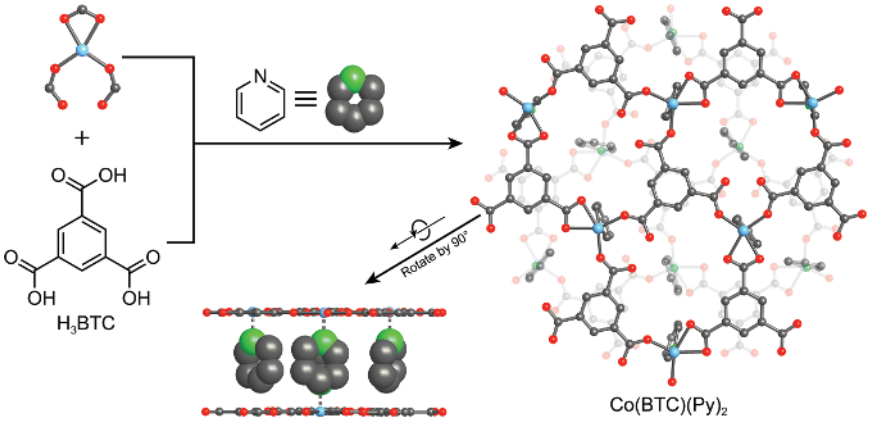

Figure 1.13 Linking Co^{3+} ions and BTC results in the formation of a layered 2D structure of formula $Co(BTC)(Py)_2$. The layers are constructed from square planar Co^{3+} and trigonal planar BTC linkers and are stacked along the crystallographic *c*-axis. The individual layers are separated by pyridine ligands coordinated to give Co^{3+} centers to given an overall octahedral coordination geometry. The pyridine guest molecules can be removed thermally and reinserted, regenerating the original structure of MOF-1 of the original structure of MOF-1. Color code: Co, blue; C, gray; N, green; O, red.

1.7 Introduction of Secondary Building Units and Permanent Porosity

To further increase the stability of metal-organic extended structures, polynuclear clusters, commonly referred to as secondary building units (SBUs), were sought as nodes to replace the single metal-ion nodes in coordination networks. The SBUs offered several advantages toward realizing more robust structures: the chelation of metal ions to make polynuclear clusters provided for rigidity and directionality while the charge on the linker led to increased bond strength and the formation of neutral frameworks. In combination, these factors were expected to contribute greatly to the overall stability of the resulting material. This concept was realized in 1998 when the synthesis and gas sorption properties of the first metal-organic framework, MOF-2 $Zn(BDC)(H_2O)$ were reported (Figure 1.14). MOF-2 has a neutral framework structure and is synthesized by slow vapor diffusion of a mixture of trimethylamine/toluene into a DMF/toluene solution of $Zn(NO_3)_2{\cdot}6H_2O$ and benzenedicarboxylic acid (H_2BDC) [33]. The layered structure of MOF-2 is built from dimeric $Zn_2(—COO)_4$ paddle wheel SBUs (rather than single metal nodes) that are linked by BDC struts to form a square grid (**sql**).

The increased stability imparted by the paddle wheel SBUs made it possible to remove all solvent molecules from the pores without collapsing the structure of MOF-2, leading to permanent microporosity as evidenced by reversible nitrogen gas adsorption at 77 K. The proof of permanent porosity in this MOF signaled a turning point in the chemistry of extended metal-organic solids and led to the use of the term MOF to emphasize their distinct stability and porosity.

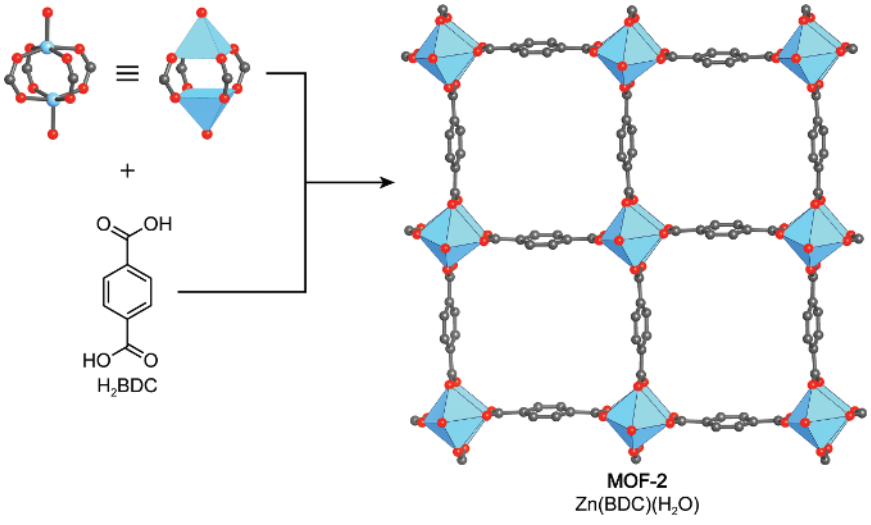

Figure 1.14 Crystal structure of MOF-2 viewed along the crystallographic *a*-axis, emphasizing the trapezoidal channels. Dinuclear Cu^{2+} paddle wheel SBUs are connected by ditopic BDC linkers to form layers of **sql** topology. The architecturally stable combination of paddle wheel SBUs and charged chelating linkers endow MOF-2 with permanent porosity. All hydrogen atoms and guest molecules are omitted for clarity. Color code: Cu, blue; C, gray; N, green; O, red.

Furthermore, this development led to extensive work on combining metals with carboxylates and other charged chelating linkers to give crystalline frameworks with SBUs as nodes. The term MOF has been overwhelmingly applied to distinguish such structures and henceforth we will adopt this terminology. The discovery of permanent porosity in MOF-2 generated interest in the further development of MOFs as it indicated that it is possible to make a wide range of 2D and 3D MOFs by combining different inorganic SBUs and organic linkers.

1.8 Extending MOF Chemistry to 3D Structures

The inorganic SBUs are polynuclear clusters in which the positions of the metal ions are locked in place by the binding groups of the linkers (in this book mainly carboxylates) as exemplified by the di-nuclear $M_2(CH_3COO)_4$ (M^{2+} = Cu, Zn) paddle wheel complex [34]. Their geometry and connectivity can be varied in order to allow for the formation of a variety of different MOF structures. These features, along with rigidity, and definitive directionality and connectivity facilitate the possibility for reticular synthesis and for the design of new, rigid, and permanently porous frameworks adopting a targeted structure. The synthetic and structural chemistry of polynuclear metal carboxylate clusters was well developed early on and many of their structures were solved soon after the discovery of X-ray diffraction by crystals [35]. As a matter of fact, the structure of the acetate capped paddle wheel clusters, as is found in the structure of MOF-2, was determined as early as 1953 [35g]. Based on the presumption that the replacement of

the capping acetate ligands with multifunctional organic molecules promotes the formation of open extended framework structures, the idea of employing other carboxylate clusters as SBUs in the formation of MOFs emerged. First attempts to extend the chemistry of MOFs into 3D involved the use of the basic zinc acetate, a tetra-nuclear carboxylate cluster coordinated by six acetates in an octahedral fashion, as an SBU [35f].

1.8.1 Targeted Synthesis of MOF-5

It was known by that time that basic zinc acetate $Zn_4O(CH_3COO)_6$ can be prepared by adding small amounts of hydrogen peroxide to a solution of a zinc salt in acetic acid [36]. This facilitates the formation of O^{2-}, which lies at the center of the resulting polynuclear cluster [37]. The knowledge of both, the synthesis route affording the molecular $Zn_4O(CH_3COO)_6$ cluster as well as that employed in the preparation of MOF-2, allowed for the deduction of a synthetic procedure targeting a 3D MOF based on octahedral $Zn_4O(—COO)_6$ SBUs and ditopic linear linkers.

One of the lessons learned from the synthesis of MOF-2 was that precise synthetic control is required in order to avoid the rapid precipitation of ill-defined amorphous powders as a result of the low reversibility of the formation of strong metal–carboxylate bonds. This is in stark contrast to structures held together by relatively weak metal–N–donor bonds (e.g. bipyridines and dinitriles) whose crystallization is relatively straightforward owing to the high reversibility and facile error correction during crystallization. In the case of MOF-2, the formation of a crystalline material was achieved by slow diffusion of a base (trimethylamine) into a solution of a mixture of the metal salt ($Zn(NO_3)_3{\cdot}6H_2O$) and the organic linker H_2BDC (benzenedicarboxylic acid). Slow deprotonation of the carboxylic acid groups of the linker slowed down the formation of MOF-2 and allowed for error correction and consequently the crystallization of MOF-2. This strategy was largely retained in the synthesis of MOF-5 and only modified by adding a small amount of hydrogen peroxide to a mixture of $Zn(NO_3)_2{\cdot}4H_2O$ and H_2BDC in analogy to the synthesis of the molecular $Zn_4O(CH_3COO)_6$ cluster, to favor the formation $Zn_4O(—COO)_6$ SBUs over the previously obtained $Zn_2(—COO)_4$ paddle wheel units.

Despite the rational approach to the synthesis of MOF-5, the bulk material that collected on the bottom of the vial turned out to be MOF-2.[6] One of the authors recalls that following this procedure, his student observed a small amount of cube-shaped crystals, having a morphology different from the main phase collecting at the bottom of the reaction vessel. These cubic crystals were floating at the meniscus of the mother liquor and adhered to the sides of the flask in the

6 Solvothermal methods to prepare MOF-5 in high yield were established in the following years where the slow diffusion of base into the reaction mixture was replaced by using DMF (dimethylformamide) or DEF (diethylformamide), which slowly decompose upon heating to release small amounts of dimethyl- or diethylamine base. It was also shown that the use of hydrogen peroxide is not needed since O^{2-} ions can be formed from trace amounts of water in the reaction mixture. Typical reaction temperatures of 80–100 °C as well as the applicability of this route to different metal salts were reported [38].

same vicinity. The comparison of the powder X-ray diffraction pattern of MOF-2 and that of these cubic crystals confirmed the presence of two structurally distinct compounds. However, when attempting to mount these cubic crystals on a single crystal X-ray diffractometer, the formation of cracks and the loss of transparency were observed, indicating the loss of mono-crystallinity and thus initially precluding their structural characterization. It proved difficult to handle this material because the crystals degraded upon loss of solvent by evaporation after they were removed from the mother liquor. Eventually, the structure of MOF-5 was determined by keeping the crystals in the mother liquor and sealing them in a capillary prior to examination by single crystal X-ray diffraction.

1.8.2 Structure of MOF-5

The synthesis, characterization, and structure of MOF-5, $[Zn_4O(BDC)_3](DMF)_x$ was reported in 1999 by Yaghi and coworkers.[7] It was shown that the structure of MOF-5 is indeed composed of octahedral $Zn_4O(—COO)_6$ SBUs, consisting of four tetrahedral ZnO_4 units sharing a common vertex, joined by ditopic BDC linkers to give a 3D framework structure of **pcu** topology (Figure 1.15). The large size (8.9 Å) and high connectivity of the SBUs in combination with the long BDC linker (6.9 Å) provide for an open porous structure with alternating interconnected pores of 15.1 and 11.0 Å in diameter, and a pore aperture of 8.0 Å.

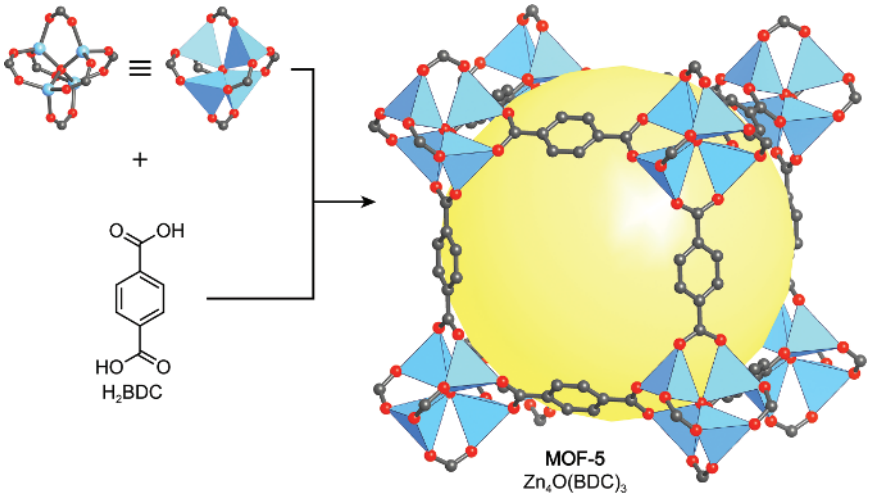

Figure 1.15 Crystal structure of MOF-5, constructed from octahedral $Zn_4O(—COO)_6$ SBUs and linear ditopic BDC linkers. The resulting primitive cubic net (**pcu**) has alternating large (15.1 Å diameter) and small (11.0 Å diameter) pores whose different size is a result of the orientation of the phenyl units of the BDC linkers with respect to the center of the pore. Only the large pore is shown for clarity. The yellow sphere indicates the largest sphere that can be placed inside the pore without coming within the van der Waals radius of any framework atom. All hydrogen atoms are omitted for clarity. Color code: Zn, blue; C, gray; O, red.

7 The name MOF-5 was chosen in analogy to the well-known zeolite ZMS-5.

These large cavities make up 61% of the unit cell volume and are filled with solvent molecules (DMF) in the as-synthesized material. One of the most striking features of the MOF-5 structure is that the pores have no walls. This provides for an unprecedented openness of the structure that allows guest molecules to move with great facility without clogging the pores. In contrast, the pores in more traditional porous solids such as zeolites have walls and diffusion can be subject to complications related to blocked pores. The structure of MOF-5 is shown in Figure 1.15 and the open space within this structure is illustrated by a yellow sphere that represents the largest sphere that can occupy the pore without penetrating the van der Waals radius of any framework atom. We will use these spheres to highlight the accessible open space within the structures of all porous frameworks discussed throughout this book.

Among the very first questions to be addressed about MOF-5 was whether the guests filling the pores could be removed without collapsing the overall structure and whether, like MOF-2, MOF-5 is stable enough to support permanent porosity. Before addressing this issue, we digress slightly to enumerate the different types of stability relevant to this and other MOFs that follow.

1.8.3 Stability of Framework Structures

Chemical stability is the ability of a given material to withstand chemical treatment without any significant change in its structure. This can be evaluated by subjecting a material to different liquid or gaseous chemicals, followed by X-ray diffraction analysis to verify that the structure of the material has not been altered or degraded.

Thermal stability is the ability of a given material to withstand thermal treatment without any significant change in its structure. This can often be assessed by thermogravimetric analysis or differential-scanning-calorimetry where, upon heating the sample, an apparent mass loss or a thermal effect (exothermic or endothermic) is recorded, indicating decomposition and changes in the structure. Additionally, X-ray diffraction studies performed on the material after or during thermal treatment can provide information on whether the structure has been retained.

Mechanical stability is the ability of a given material to withstand external forces. Methods to determine the mechanical stability of MOFs are similar to those used in materials science such as pressurization (compressibility), nano-indentation (Young's modulus) or determination of the tensile strength to name a few.

Architectural stability is the ability of a framework material to retain its structural integrity in the absence of guest molecules. It can be proven by evacuating the solvent from the pores of a MOF and subsequent confirmation of its crystal structure and porosity.

1.8.4 Activation of MOF-5

To realize the full potential of MOF-5, the challenge of removing guest molecules to yield an open framework was addressed. Initial attempts to evaporate the solvent guest molecules from the crystal caused cracking and a concomitant partial loss of porosity that were ascribed to the strong mechanical forces acting on the

framework upon solvent removal. These forces are proportional to the surface tension of the solvent in the pores and the extent of the "adhesive forces" between the guest molecules and the inner surface of the MOF. To facilitate the evacuation of the material, the highly mobile guest molecules present in the pores of the as-synthesized material were fully exchanged with chloroform ($CHCl_3$), which upon removal "puts less stress on the framework." The complete removal of all guest molecules from the pores of MOF-5 was eventually achieved by evacuation of the solvent exchanged material at 5×10^{-5} Torr and room temperature for three hours with full retention of the crystallinity of the architecturally stable framework [37]. The process of removing volatile guest molecules from the pores of MOFs is commonly referred to as "activation."

Since no change in morphology or transparency was observed upon activation of MOF-5, single crystal X-ray diffraction studies of the activated material were carried out. This is usually difficult because porous solid-state materials often lose their monocrystallinity upon removal of guest molecules. However, in this case the unit cell parameters and atomic positions determined from these measurements were shown to be almost identical to those of the as-synthesized material. In fact, the remaining electron density within the pores was significantly lower than for the as-synthesized material, providing further proof that all guest molecules had been removed and that MOF-5 is indeed permanently porous[8] [37].

1.8.5 Permanent Porosity of MOF-5

The next step in proving the permanent porosity of MOF-5 was the determination of its internal surface area. For this purpose, nitrogen adsorption experiments at 77 K (as recommended by IUPAC) were performed (Figure 1.16). These measurements allow for the determination of both pore size and surface area. The pore volume calculated from these measurements (0.54–0.61 $cm^3\ cm^{-3}$) was higher than those reported for the best performing zeolites at that time (up to 0.47 $cm^3\ cm^{-3}$) [37]. With a value of 2900 $m^2\ g^{-1}$, the Langmuir surface area reported in this contribution surpassed by far that of all zeolites, activated carbons, and other porous materials.[9] In later contributions, even higher surface areas up to 3800 $m^2\ g^{-1}$ were reported as better methods for the activation of MOFs were developed [38a].

The combination of a 6-connected $Zn_4O(—COO)_6$ cluster and charged bridging carboxylate linkers suggest that the resulting framework should exhibit high thermal stability, and indeed, neither the morphology nor the crystallinity of the fully activated MOF-5 was affected by heating the material in dry air at 300 °C for 24 hours. This was further evidenced by subsequent single crystal X-ray diffraction studies carried out on MOF-5 samples that underwent this procedure [37]. Furthermore, MOF-5 was shown to be stable at temperatures up to 400 °C under vacuum. The structural degradation of MOF-5 under atmospheric conditions can

8 A material is defined as permanently porous if it is proven to be stable upon removal of the guests from the pores without collapsing. This is measured by nitrogen gas adsorption experiments (at 77 K relative pressures between 0 and 1), the gold standard for evaluation of porosity.

9 Ulrich Müller, a research director at BASF SE, recalls his reaction when he came across this study on MOF-5 and stated: "That number was so unbelievably high, I thought it had to be a misprint." Only after having repeated the measurement himself was he convinced [39].

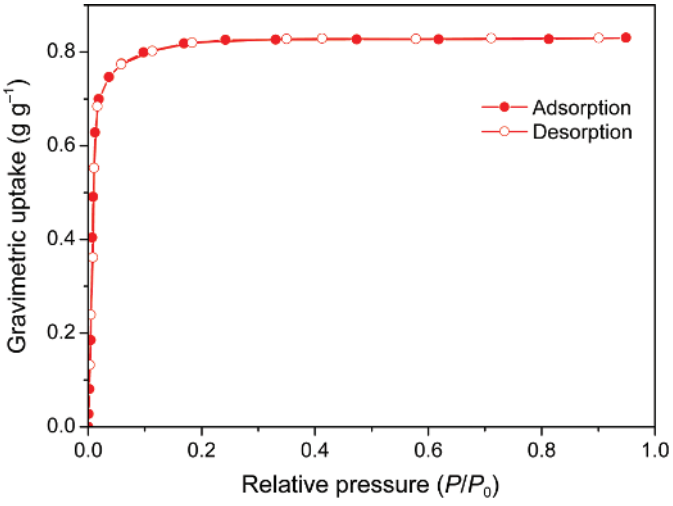

Figure 1.16 Nitrogen adsorption isotherm measured at 77 K. A pore volume of 0.54–0.61 $cm^3\ cm^{-3}$ and a Langmuir surface area of 2900 $m^2\ g^{-1}$ have been calculated from this measurement. The fact that the desorption branch perfectly traces the adsorption branch highlights the outstanding architectural and mechanical stability of MOF-5 and gives further evidence of its permanent porosity.

therefore be ascribed to humidity in the air rather than to oxygen. This is further supported by the fact that treating MOF-5 with dry solvents or dry air has no effect on its crystallinity and surface area, whereas treatment with humid air or moist solvents results in the slow decomposition of MOF-5 and the formation of a nonporous product [38a].

1.8.6 Architectural Stability of MOF-5

It is worthy of note, that when MOF-5 was first reported, there were many doubters as no one expected such an open structure, composed of largely open space, to be architecturally and thermally stable. Many expected the framework to collapse onto itself once the solvent guests are removed. To gain a deeper understanding of the key factors rendering MOF-5 architecturally stable, it is helpful to take a closer look at its structure. The cubic structure of MOF-5 (Figure 1.17a) can be deconstructed into the basic **pcu** net, that is, a framework built from single atom vertices connected by edges (Figure 1.17b). When a shear force is applied to this basic **pcu** net little resistance is expected. This however does not hold true for the actual crystal structure of MOF-5. In its crystal structure, the vertices of the basic **pcu** net are cationic zinc-oxide clusters that have an envelope[10] of truncated tetrahedral shape. These vertices are joined together by the rigid planar BDC linkers, which can be represented by a planar flat envelope (Figure 1.17c). Each set of linkers located on opposing sides of the truncated

10 The envelope representation of individual building units in carboxylate MOFs are geometrical shapes identical to those obtained when wrapping the respective building units in paper (thus envelope) while making sure, that all oxygen atoms of the carboxylate groups are touching the paper.

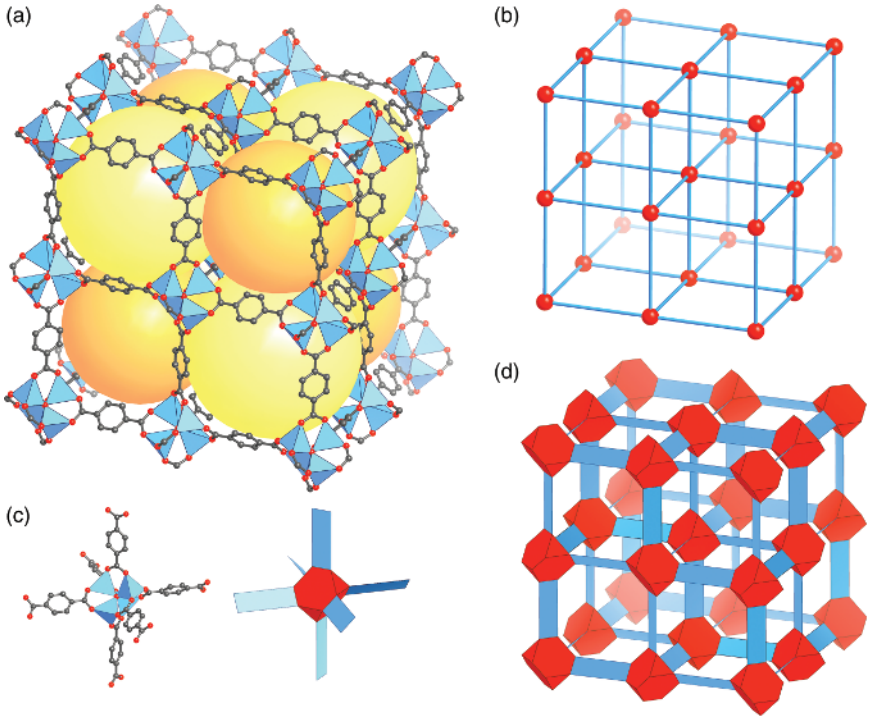

Figure 1.17 (a) Crystal structure of MOF-5, the two differently sized pores are highlighted by yellow (large pore, 15.1 Å diameter) and orange spheres (small pore, 11.0 Å), respectively. (b) Simplified representation of the basic **pcu** net of MOF-5. SBUs are replaced by single atom vertices and the BDC linkers are replaced by edges. (c) Envelope representation of the octahedral $Zn_4O(—COO)_6$ SBUs and the BDC linker as truncated tetrahedra and rectangles, respectively. (d) Envelope representation of the extended framework structure of MOF-5, highlighting its architectural stability that originates from the mutually perpendicular arrangement of BDC linkers around the SBUs. Color code: Zn, blue tetrahedra; C, gray; O, red. In the topology and envelope representation, nodes are shown in red, linkers in blue.

tetrahedron has a dihedral angle of 90°; i.e. they are rotated by 90° with respect to each other. Linking these two building units into an extended 3D framework results in an inherently rigid structure, held together by mutually perpendicular hinges (Figure 1.17d). This arrangement provides for the high architectural stability needed to allow for the activation and support of permanent porosity. The high thermal stability of MOF-5 on the other hand is attributed to the fact that the backbone of MOF-5 is composed entirely of strong bonds (Zn—O, C—O, and C—C), all of which are significantly stronger and therefore thermodynamically more stable than those in coordination networks (M–N–donor) [40].

1.9 Summary

In this chapter we have outlined the history of the development of MOFs. We showed the transition from 0D amine and nitrile-based coordination compounds

into 2D and 3D coordination networks and highlighted the key points in making robust, chemically, mechanically, and architecturally stable compounds that support permanent porosity: (i) The use of charged chelating linker and (ii) the SBU approach. In this way, the need for counter ions that reside in the pores of the framework can be avoided, and the rigidity of the building units – organic linker and SBU – renders the framework architecturally stable. We showed that different SBUs can be targeted in a rational manner, thus presenting the prospect of the designed synthesis of a vast variety of possible framework structures. In the following chapters we will consider the porosity of such frameworks in more detail.

References

1 (a) Kraft, D.A. (2012). *Wege des Wissens: Berliner Blau, 1706–1726.*; Frankfurt/Main: Gesellschaft Deutscher Chemiker/Fachgruppe Geschichte der Chemie. Bd 22. ISSN 0934-8506. https://www.gdch.de/fileadmin/downloads/Netzwerk_und_Strukturen/Fachgruppen/Geschichte_der_Chemie/Mitteilungen_Band_22/2012-22-02.pdf (b) Ball, P. (2003). *Bright Earth: Art and the Invention of Color*. Penguin. (c) Bartoll, J. (2008). Proceedings of the 9th International Conference on NDT of Art https://www.ndt.net/article/art2008/papers/029bartoll.pdf.

2 Stahl, G. (1731). Experimenta, observationes, animadversiones. *Chymicae et Physicae (Berlin)* 300: 281–283.

3 (a) Orna, M.V., Kozlowski, A.W., Baskinger, A., and Adams, T. (1994). *Coordination Chemistry: A Century of Progress*, American Chemical Society Symposium Series 565, 165–176. Washington, DC: American Chemical Society. (b) Wunderlich, C.-H. and Bergerhoff, G. (1994). Konstitution und Farbe von Alizarin- und Purpurin-Farblacken. *Chemische Berichte* 127 (7): 1185–1190.

4 (a) Kauffman, G.B. (2013). *Alfred Werner: Founder of Coordination Chemistry*. Springer Science & Business Media. (b) Constable, E.C. and Housecroft, C.E. (2013). Coordination chemistry: the scientific legacy of Alfred Werner. *Chemical Society Reviews* 42 (4): 1429–1439.

5 Werner, A. (1893). Beitrag zur konstitution anorganischer verbindungen. *Zeitschrift für Anorganische Chemie* 3 (1): 267–330.

6 (a) Kekulé, A. (1857). Ueber die sg gepaarten Verbindungen und die Theorie der mehratomigen Radicale. *European Journal of Organic Chemistry* 104 (2): 129–150. (b) Kekulé, A. (1858). Über die Constitution und die Metamorphosen der chemischen Verbindungen und über die chemische Natur des Kohlenstoffs. *European Journal of Organic Chemistry* 106 (2): 129–159.

7 (a) Blomstrand, C.W. (1869). *Chemie der Jetztzeit*. Heidelberg: C. Winter. (b) Jörgensen, S. (1894). Zur Konstitution der Kobalt-, Chrom-und Rhodiumbasen. *Zeitschrift für Anorganische und Allgemeine Chemie* 5 (1): 147–196. (c) Kauffman, G.B. (1959). Sophus Mads Jorgensen (1837–1914): a chapter in coordination chemistry history. *Journal of Chemical Education* 36 (10): 521–527.

8 Werner, A. and Miolati, A. (1894). *Zeitschrift für Physik Chem Leipzig* 14: 506–511.

9 Werner, A. (1907). Über 1.2-Dichloro-tetrammin-kobaltisalze. (Ammoniak-violeosalze). *European Journal of Inorganic Chemistry* 40 (4): 4817–4825.

10 Hofmann, K. and Küspert, F. (1897). Verbindungen von kohlenwasserstoffen mit metallsalzen. *Zeitschrift für Anorganische Chemie* 15 (1): 204–207.

11 Powell, H.M. (1948). 15. The structure of molecular compounds. Part IV. Clathrate compounds. *Journal of the Chemical Society (Resumed)* 61–73.

12 Rayner, J. and Powell, H.M. (1952). 67. Structure of molecular compounds. Part X. Crystal structure of the compound of benzene with an ammonia–nickel cyanide complex. *Journal of the Chemical Society (Resumed)* 319–328.

13 (a) Iwamoto, T., Miyoshi, T., Miyamoto, T. et al. (1967). The metal ammine cyanide aromatics clathrates. I. The preparation and stoichiometry of the diamminemetal(II) tetracyanoniccolate(II) dibenzene and sianiline. *Bulletin of the Chemical Society of Japan* 40 (5): 1174–1178. (b) Iwamoto, T., Nakano, T., Morita, M. et al. (1968). The Hofman-type clathrate: $M(NH_3)_2M'(CN)_4$. 2G. *Inorganica Chimica Acta* 2: 313–316. (c) Miyoshi, T., Iwamoto, T., and Sasaki, Y. (1972). The structure of catena-μ-ethylenediaminecadmium(II)tetracyanoniccolate(II)dibenzene clathrate: $Cd(en)Ni(CN)_4{\cdot}2C_6H_6$. *Inorganica Chimica Acta* 6: 59–64. (d) Walker, G. and Hawthorne, D. (1967). Complexes between n-alkylamines and nickel cyanide. *Transactions of the Faraday Society* 63: 166–174.

14 Nishikiori, S.-I. and Iwamoto, T. (1984). Crystal structure of Hofmann-dma-type benzene clathrate bis(dimethylamine)cadmium(II) tetracyanonickelate(II) benzene(2/1). *Chemistry Letters* 13 (3): 319–322.

15 (a) Hasegawa, T., Nishikiori, S.-I., and Iwamoto, T. (1984). *Clathrate Compounds, Molecular Inclusion Phenomena, and Cyclodextrins*, 351–357. Springer. (b) Hasegawa, T., Nishikiori, S.-I., and Iwamoto, T. (1985). Isomer selection of 1,6-diaminohexanecadmium(II) tetracyznonickelate(II) for *m*- and *p*-toluidine. Formation of 1,6-diaminohexanecadmium(II) tetracyznonickelate(II) *m*-toluidine (1/1) inclusion compound and bis(*p*-toluidine)-1,6-diaminohexanecadmium(II)tetracyznonickelate(II) complex. *Chemistry Letters* 14 (11): 1659–1662. (c) Nishikiori, S.-I., Hasegawa, T., and Iwamoto, T. (1991). The crystal structures of α,ω-diaminoalkanecadmium(II) tetracyanonickelate(II) aromatic molecule inclusion compounds. V. Toluidine clathrates of the hosts built of the diamines, 1,4-diaminobutane, 1,5-diaminonentane, and 1,8-diaminooctane. *Journal of Inclusion Phenomena and Molecular Recognition in Chemistry* 11 (2): 137–152.

16 (a) Kinoshita, Y., Matsubara, I., and Saito, Y. (1959). The crystal structure of bis(succinonitrilo)copper(I) nitrate. *Bulletin of the Chemical Society of Japan* 32 (7): 741–747. (b) Kinoshita, Y., Matsubara, I., and Saito, Y. (1959). The crystal structure of bis(glutaronitrilo)copper(I) nitrate. *Bulletin of the Chemical Society of Japan* 32 (11): 1216–1221. (c) Kinoshita, Y., Matsubara, I., Higuchi, T., and Saito, Y. (1959). The crystal structure of

bis(adiponitrilo)copper(I) nitrate. *Bulletin of the Chemical Society of Japan* 32 (11): 1221–1226.

17 Wells, A. (1954). The geometrical basis of crystal chemistry. Part 1. *Acta Crystallographica* 7 (8–9): 535–544.

18 Ockwig, N.W., Delgado-Friedrichs, O., O'Keeffe, M., and Yaghi, O.M. (2005). Reticular chemistry: occurrence and taxonomy of nets and grammar for the design of frameworks. *Accounts of Chemical Research* 38 (3): 176–182.

19 Aumüller, A., Erk, P., Klebe, G. et al. (1986). A radical anion salt of 2,5-dimethyl-*N*,*N*′-dicyanoquinonediimine with extremely high electrical conductivity. *Angewandte Chemie International Edition in English* 25 (8): 740–741.

20 Kato, R., Kobayashi, H., and Kobayashi, A. (1989). Crystal and electronic structures of conductive anion-radical salts,(2,5-R_1R_2-DCNQI)$_2$Cu (DCNQI = *N*,*N*′-dicyanoquinonediimine; R_1, R_2 = CH_3, CH_3O, Cl, Br). *Journal of the American Chemical Society* 111 (14): 5224–5232.

21 Desiraju, G.R. and Parshall, G.W. (1989). *Crystal Engineering: The Design of Organic Solids*, Materials Science Monographs, vol. 54. Elsevier.

22 Moulton, B. and Zaworotko, M.J. (2001). From molecules to crystal engineering: supramolecular isomerism and polymorphism in network solids. *Chemical Reviews* 101 (6): 1629–1658.

23 (a) Zhdanov, H. (1941). The crystalline structure of $Zn(CN)_2$. *Comptes Rendus de l'Académie des Sciences de l'URSS* 31: 352–354. (b) Shugam, E. and Zhdanov, H. (1945). The crystal structure of cyanides. II. The structure of $Cd(CN)_2$. *Acta Physicochim. URSS* 20: 247–252. (c) Takafumi, K., Shin-ichi, N., Reiko, K., and Toschitake, I. (1988). Novel clathrate compound of cadmium cyanide host with an adamantane-like cavity. Cadmium cyanide–carbon tetrachloride(1/1). *Chemistry Letters* 17 (10): 1729–1732.

24 (a) Hoskins, B.F. and Robson, R. (1989). Infinite polymeric frameworks consisting of three dimensionally linked rod-like segments. *Journal of the American Chemical Society* 111 (15): 5962–5964. (b) Hoskins, B. and Robson, R. (1990). Design and construction of a new class of scaffolding-like materials comprising infinite polymeric frameworks of 3D-linked molecular rods. A reappraisal of the zinc cyanide and cadmium cyanide structures and the synthesis and structure of the diamond-related frameworks $[N(CH_3)_4][Cu^{I}Zn^{II}(CN)_4]$ and Cu^{I}[4,4′,4″,4‴-tetracyanotetraphenylmethane]BF_4.x$C_6H_5NO_2$. *Journal of the American Chemical Society* 112 (4): 1546–1554.

25 Zaworotko, M.J. (1994). Crystal engineering of diamondoid networks. *Chemical Society Reviews* 23 (4): 283–288.

26 Gable, R.W., Hoskins, B.F., and Robson, R. (1990). Synthesis and structure of $[NMe_4][CuPt(CN)_4]$: an infinite three-dimensional framework related to PtS which generates intersecting hexagonal channels of large cross section. *Journal of the Chemical Society, Chemical Communications* (10): 762–763.

27 Abrahams, B.F., Hoskins, B.F., Michail, D.M., and Robson, R. (1994). Assembly of porphyrin building blocks into network structures with large channels. *Nature* 369 (6483): 727–729.

28 Fujita, M., Yazaki, J., and Ogura, K. (1990). Preparation of a macrocyclic polynuclear complex, $[(en)Pd(4,4'\text{-bpy})]_4(NO_3)_8$ (en = ethylenediamine, bpy = bipyridine), which recognizes an organic molecule in aqueous media. *Journal of the American Chemical Society* 112 (14): 5645–5647.

29 Fujita, M., Kwon, Y.J., Washizu, S., and Ogura, K. (1994). Preparation, clathration ability, and catalysis of a two-dimensional square network material composed of cadmium(II) and 4,4′-bipyridine. *Journal of the American Chemical Society* 116 (3): 1151–1152.

30 Yaghi, O. and Li, H. (1995). Hydrothermal synthesis of a metal-organic framework containing large rectangular channels. *Journal of the American Chemical Society* 117 (41): 10401–10402.

31 Subramanian, S. and Zaworotko, M.J. (1995). Porous solids by design: $[Zn(4,4'\text{-bpy})_2(SiF_6)]_n \cdot xDMF$, a single framework octahedral coordination polymer with large square channels. *Angewandte Chemie International Edition in English* 34 (19): 2127–2129.

32 Yaghi, O.M., Li, G., and Li, H. (1995). Selective binding and removal of guests in a microporous metal-organic framework. *Nature* 378 (6558): 703.

33 Li, H., Eddaoudi, M., Groy, T.L., and Yaghi, O.M. (1998). Establishing microporosity in open metal-organic frameworks: gas sorption isotherms for Zn(BDC) (BDC = 1,4-Benzenedicarboxylate). *Journal of the American Chemical Society* 120 (33): 8571–8572.

34 Tranchemontagne, D.J., Mendoza-Cortes, J.L., O'Keeffe, M., and Yaghi, O.M. (2009). Secondary building units, nets and bonding in the chemistry of metal-organic frameworks. *Chemical Society Reviews* 38 (5): 1257–1283.

35 (a) Bragg, W.L. (1914). Die Beugung kurzer elektromagnetischer Wellen durch einen Kristall. *Zeitschrift für Anorganische Chemie* 90 (1): 153–168. (b) Friedrich, W., Knipping, P., and Laue, M. (1913). Interferenzerscheinungen bei Röntgenstrahlen. *Annalen der Physik* 346 (10): 971–988. (c) Komissarova, L.N., Simanov, Y.P., Plyushchev, Z.N., and Spitsyn, V.I. (1966). Zirconium and hafnium oxoacetates. *Russian Journal of Inorganic Chemistry* 11 (9): 2035–2040. (d) Komissarova, L.N.K., Prozorovskaya, S.V., Plyushchev, Z.N., and Plyushchev, V.E. (1966). Zirconium and hafnium oxoacetates. *Russian Journal of Inorganic Chemistry* 11 (2): 266–271. (e) Koyama, H. and Saito, Y. (1954). The crystal structure of zinc oxyacetate, $Zn_4O(CH_3COO)_6$. *Bulletin of the Chemical Society of Japan* 27 (2): 112–114. (f) van Niekerk, J.N., Schoening, F.R.L., and Talbot, J.H. (1953). The crystal structure of zinc acetate dihydrate, $Zn(CH_3COO)_2 \cdot 2H_2O$. *Acta Crystallographica* 6 (8–9): 720–723. (g) van Niekerk, J.N. and Schoening, F.R.L. (1953). X-ray evidence for metal-to-metal bonds in cupric and chromous acetate. *Nature* 171 (4340): 36–37.

36 Lionelle, J.E. and Staffa, J.A. (1983). Metal oxycarboxylates and method of making same. US Patent US10596310.

37 Li, H., Eddaoudi, M., O'Keeffe, M., and Yaghi, O.M. (1999). Design and synthesis of an exceptionally stable and highly porous metal-organic framework. *Nature* 402 (6759): 276–279.

38 (a) Kaye, S.S., Dailly, A., Yaghi, O.M., and Long, J.R. (2007). Impact of preparation and handling on the hydrogen storage properties of

Zn_4O(1,4-benzenedicarboxylate)$_3$ (MOF-5). *Journal of the American Chemical Society* 129 (46): 14176–14177. (b) Tranchemontagne, D.J., Hunt, J.R., and Yaghi, O.M. (2008). Room temperature synthesis of metal-organic frameworks: MOF-5, MOF-74, MOF-177, MOF-199, and IRMOF-0. *Tetrahedron* 64 (36): 8553–8557.

39 Jacoby, M. (2008). Heading to market with MOFs. *Chemical and Engineering News* 86 (34): 13–16.

40 (a) Yaghi, O.M., O'Keeffe, M., Ockwig, N.W. et al. (2003). Reticular synthesis and the design of new materials. *Nature* 423 (6941): 705–714. (b) Kiang, Y.-H., Gardner, G.B., Lee, S. et al. (1999). Variable pore size, variable chemical functionality, and an example of reactivity within porous phenylacetylene silver salts. *Journal of the American Chemical Society* 121 (36): 8204–8215. (c) Jiang, J., Zhao, Y., and Yaghi, O.M. (2016). Covalent chemistry beyond molecules. *Journal of the American Chemical Society* 138 (10): 3255–3265.